Dyes and Pigments 99 (2013) 1010–1015

Contents lists available at ScienceDirect

Dyes and Pigments

journal homepage: www.elsevier.com/locate/dyepig

Greenish yellow organic light emitting devices based on novel iridium complexes containing 2-cyclohexenyl-1-phenyl-1*H*-benzo[*d*]imidazole

Liangliang Han [a], Dongyu Zhang [b], Yuanhang Zhou [a], Ying Yang [a], Han Young Woo [c], Fali Bai [a], Renqiang Yang [a,*]

[a] *Qingdao Institute of Bioenergy and Bioprocess Technology, Chinese Academy of Sciences, Qingdao 266101, China*
[b] *Suzhou Institute of Nano-Tech and Nano-Bionics, Chinese Academy of Sciences, Suzhou 215123, China*
[c] *Department of Cogno-Mechatronics Engineering (WCU), Pusan National University, Miryang 627-706, South Korea*

ARTICLE INFO

Article history:
Received 7 June 2013
Received in revised form
8 August 2013
Accepted 13 August 2013
Available online 26 August 2013

Keywords:
Organic light emitting devices
Greenish yellow phosphorescence
2-Cyclohexenyl-1-phenyl-1*H*-benzo[*d*]imidazole
Heterocyclometalated iridium complexes
Photoluminescence
Electroluminescence

ABSTRACT

2-Cyclohexenyl-1-phenyl-1*H*-benzo[*d*]imidazole (Hcyclopbi) and its heterocyclometalated iridium complexes bis[2-cyclohexenyl-1-phenyl-1*H*-benzo[*d*]imidazole](acetylacetonate)iridium(III) [(cyclopbi)$_2$Iracac] and bis[2-cyclohexenyl-1-phenyl-1*H*-benzo[*d*]imidazole][2-(3-(trifluoromethyl)-1*H*-pyrazol-5-yl)pyridinate]iridium(III) [(cyclopbi)$_2$IrCF$_3$] were firstly designed and synthesized. Owing to the strong electron withdrawing ability of 2-(3-(trifluoromethyl)-1*H*-pyrazol) compared to that of acetylacetonate, blue shifted phosphorescence 542 nm was obtained for (cyclopbi)$_2$IrCF$_3$ compared to that of (cyclopbi)$_2$Iracac 545 nm with photoluminescence quantum yields (φ) 0.22 and 0.25, respectively, as well the highest occupied molecular orbit (HOMO) energy level was estimated to be −5.10 eV for (cyclopbi)$_2$IrCF$_3$, 0.19 eV lower than that of −4.91 eV for (cyclopbi)$_2$Iracac. When (cyclopbi)$_2$Iracac was doped into 4,4′-bis(9*H*-carbazol-9-yl)biphenyl (CBP) as the emitting layer, high efficiency organic light emitting devices (OLEDs) were obtained with maximum current efficiency (η_c) 22.3 cd/A at 3.1 mA/cm^2 and maximum brightness 16,300 cd/m^2 at 171.6 mA/cm^2, which were comparable to those of bis(2-phenylpyridine)(acetylacetonate)iridium(III) [(ppy)$_2$Iracac] with the same device structure. This results indicate that (cyclopbi)$_2$Iracac and (cyclopbi)$_2$IrCF$_3$ are potential phosphorescent dyes used for OLEDs.

1. Introduction

Organic light emitting devices (OLEDs) are currently an active research area due to their potential applications in flat-panel displays and solid-state lightings [1–5]. Ir(III) complexes have attracted much attentions on improving OLEDs' efficiency because the close-lying $\pi-\pi^*$ and metal to ligand charge transfer (MLCT) states in these complexes together with the heavy atom effect enhance the spin-orbit coupling, which result in utilization both singlet and triplet excitons, causing nearly one unity of internal quantum efficiency [5–9]. Alkenyl-heterocyclic ligands were easily to obtain low energy phosphorescence in their cyclometalated iridium complexes with high photoluminescence (PL) and electroluminescence (EL) quantum efficiency which have been widely studied during the past decades. Styrylpyridine, styrylquinoline, styrylisoquinoline were firstly employed as cyclometalated ligands and used for OLEDs application with maximum current efficiency (η_c) 43.9 cd/A by Cheng and co-workers [10–12]. According to our work [13], through changing the ancillary ligand, heterocyclometalated iridium complexes containing syrylbenzothiazole show saturated red phosphorescence with Commission International de l'Eclairage (CIE) coordinates (0.64, 0.36), which were also reported by Xiao et al. [14]. As well as known iridium complexes based on 1-phenyl-1*H*-benzo[*d*]imidazole were one of the most efficient phosphores with high electron mobility which was firstly reported by Lin and co-workers in 2004 [15–17]. Followed by the styrylbenzoimidazole derivatives and their iridium complexes, high efficiency OLEDs were obtained comparable to that of tris(2-phenylpyridine)iridium [Ir(ppy)$_3$] [18]. However, styryl-heterocyclic derivatives always show lower triplet energy compared to that of phenyl-heterocyclic derivatives because of the increased conjugation length, which lead to orange or red phosphorescence for their iridium complexes. Kang et al. [19,20] have employed yellowish green iridium complex tris[2-(1-cyclohexenyl)

---

* Corresponding author. Fax: +86 532 80662778.
E-mail address: yangrq@qibebt.ac.cn (R. Yang).

0143-7208/$ – see front matter © 2013 Elsevier Ltd. All rights reserved.
http://dx.doi.org/10.1016/j.dyepig.2013.08.011

pyridine]iridium [Ir(chpy)$_3$] as the phosphors which exhibit high EL external quantum efficiency 18.7% higher than that of Ir(ppy)$_3$ without influence the triplet energy significantly. The highest occupied molecular orbital (HOMO) and the lowest unoccupied molecular orbital (LUMO) of Ir(chpy)$_3$ were higher than that of the host which result as more balanced hole and electron mobility in the emitting layer (EML). Taking into account 1-phenyl-1*H*-benzo[*d*]imidazole show higher electron mobility than that of pyridine derivatives and better stability of cyclohexenyl-heterocyclic than styryl-heterocyclic derivatives [21]. Thus the designing of cyclohexenyl-benzoimidazole ligand and its iridium complex are expected to obtain high efficiency phosphorescent organic light emitting devices (PhOLEDs).

In this article we designed novel alkenyl-benzoimidazole derivative 2-cyclohexenyl-1-phenyl-1*H*-benzo[*d*]imidazole (Hcyclopbi), which was simply synthesized by condensation of *N*-phenyl-*o*-phenylenediamine and cyclohexene-1-carbaldehyde. Heterocyclo metalated iridium complexes bis[2-cyclohexenyl-1-phenyl-1*H*-benzo[*d*]imidazole](acetylacetonate)iridium(III) [(cyclopbi)$_2$Iracac] and bis[2-cyclohexenyl-1-phenyl-1*H*-benzo[*d*]imidazole][2-(3-(trifluoromethyl)-1*H*-pyrazol-5-yl)pyridinate]iridium(III) [(cyclopbi)$_2$IrCF$_3$] were also synthesized as greenish-yellow phosphorescent dyes. When (cyclopbi)$_2$Iracac was doped into 4,4′-bis(9*H*-carbazol-9-yl)biphenyl (CBP) as the emitting layer, maximum current efficiency (η_c) 22.3 cd/A was obtained at 3.1 mA/cm^2 and maximum brightness 16,300 cd/m^2 at 171.6 mA/cm^2, which were comparable to those of bis(2-phenylpyridine)(acetylacetonate)iridium(III) [(ppy)$_2$Iracac] with the same device structure.

2. Experimental details

2.1. Reagents and measurements

All reactions were performed under argon. Solvents were carefully dried and distilled from appropriate drying agents prior to use. Commercially available reagents were used without further purification unless otherwise stated. All reactions were monitored by using thin-layer chromatography (TLC) with Merck pre-coated glass plates. Compounds were visualized with UV-light irradiation at 254 and 365 nm. High resolution mass spectra (HRMS) were obtained using a Bruker Maxis UHR-TOF, Ion Source: APCI system. Nuclear magnetic resonance (NMR) spectra were measured in appropriate deuterated solvents (CDCl$_3$ or DMSO-d_6) on a Bruker AVANCE 600 MHz Fourier transform NMR spectrometer; chemical shifts were quoted relative to the internal standard tetramethylsilane for ^{1}H NMR data. Absorption and photoluminescence spectra were measured with a Hitachi U-4100 UV–Vis–NIR scanning spectrophotometer and HORIBA JOBIN YVON FluoroMax-4 spectrophotometer, respectively. The electrochemistry characteristics of the two complexes were investigated using a cyclic voltammetry employing a diameter of 3 mm glass carbon electrode as working electrode, a platinum wire as counter electrode and an Ag/AgCl (3.0 M KCl) electrode as reference electrode. The cyclic voltammograms were obtained from a one-compartment glass cell in dichloromethane containing 10^{-3} M iridium complexes and 0.1 M tetra(*n*-butyl)ammonium hexafluorophosphate (n-Bu$_4$NPF$_6$) as a supporting electrolyte, where the scan rate was 100 mV s^{-1}, the HOMO and LUMO energy level was calculated as the reference method [18].

2.2. Device fabrication and measurement

OLEDs were grown on a glass substrate pre-coated with a ~130-nm-thick indium-tin-oxide (ITO) layer with a sheet resistance of ~20 Ω/□. Prior to organic layer deposition, the substrate was degreased with solvents and cleaned for 5 min by exposure to an UV-ozone ambient, then it was immediately loaded into the evaporation system. With a base pressure of $\sim 3 \times 10^{-4}$ Pa, the organic and metal cathode layers were grown successively by using an in vacuo mask exchange mechanism without breaking vacuum. Firstly, a 10-nm-thick 4,4′,4″-tris(*N*-3-methylphenyl-*N*-phenyl-amino)triphenylamine (m-MTDATA) hole injection layer (HIL) was deposited, followed by a 20-nm-thick 4,4′-bis[*N*-(1-naphthyl)-*N*-phenyl-amino]biphenyl (NPB) hole transporting layer (HTL). Then a 30-nm-thick EML consisting of various weight ratio iridium complexes doped into a 4,4′-bis(9*H*-carbazol-9-yl)biphenyl (CBP) host was prepared via thermal codeposition. Next, a 30-nm-thick 1,3,5-tri(1-phenyl-1*H*-benzo[*d*]imidazol-2-yl)phenyl (TPBi) layer was used to block hole and transport electron. A shadow mask with rectangular 2 mm × 2 mm openings was used to define the cathode consisting of a 1-nm-thick LiF layer, followed by a 100-nm-thick Al layer. The EL spectra were recorded with a PR655 spectrophotometer. The brightness–current–voltage (*B*–*I*–*V*) characteristics of OLEDs were measured with Keithley 2400. All the measurements were carried out at room temperature under ambient conditions.

2.3. Synthesis

As shown in Scheme 1, the cyclometalated ligand Hcyclopbi was synthesized by condensation of *N*-phenyl-*o*-phenylenediamine and cyclohexene-1-carbaldehyde in 2-ethoxyethanol, after purified on column chromatography using dichloromethane and ethyl acetic as eluent, colorless solution and brown solid was obtained when the solvent was evaporated with satisfied yield 68.5%, which was firstly reported to our knowledge now and the structure was characterized by NMR, and HRMS. Hcyclopbi was used to react with IrCl$_3$·3H$_2$O to give cyclometalated Ir-μ-chloro-bridged dimer, which could react with acetylacetone or 2-(3-(trifluoromethyl)-1*H*-pyrazol-5-yl) pyridine to afford heterocyclometalated (cyclopbi)$_2$Iracac or (cyclopbi)$_2$IrCF$_3$, respectively, in the presence of Na$_2$CO$_3$. Both the complexes show strong phosphorescence on silica gel plates under the excitation of 365 nm. The synthesis methods are described as below:

2.3.1. 2-Cyclohexenyl-1-phenyl-1H-benzo[d]imidazole (**Hcyclopbi**)

N-phenyl-*o*-phenylenediamine (1.84 g, 10 mmol) and cyclohexene-1-carbaldehyde (1.10 g, 10 mmol) were charged into a two-neck round bottomed flask and 2-ethoxyethanol (20 ml) was added under nitrogen atmosphere. The mixture was heated at 110 °C for 24 h. The solvent was removed under vacuum and the resulting mixture was extracted into dichloromethane. The organic extract was washed with brine solution, dried over anhydrous Na$_2$SO$_4$ and filtered. After the solvent was evaporated, the crude product was purified on a silica gel column using acetic ether and dichloromethane as eluent to give the desired product as a brown solid (1.88 g, 68.5%). ^{1}H NMR (DMSO-d_6, 600 MHz): δ = 7.6869 (d, J = 7.86 Hz, 1 H), 7.6126 (t, J = 7.44 Hz, 2 H), 7.5510-7.5261 (m, 1 H), 7.4525-7.4384 (m, 2 H), 7.2543-7.1808 (m, 2 H), 7.0781 (d, J = 7.92 Hz, 1 H); HRMS (APCI): m/z calcd for C$_{19}$H$_{18}$N$_2$: 274.1470; found: 274.1515.

2.3.2. Bis[2-cyclohexenyl-1-phenyl-1H-benzo[d]imidazole](acetylacetonate)iridium(III) [**(cyclopbi)$_2$Iracac**]

Hcyclopbi (0.6 g, 2.2 mmol) was dissolved into a mixed solution of 2-ethoxyethanol (15 ml) and water (5 ml) in a 50 ml round bottomed flask, then IrCl$_3$·3H$_2$O (0.35 g, 1 mmol) was added. The mixture was stirred under nitrogen at 100 °C for 12 h. The mixture was cooled to room temperature and the precipitate was collected and washed with water, ethanol, and acetone, respectively, then dried in vacuum to give cyclometalated Ir-μ-chloro-bridged dimer.

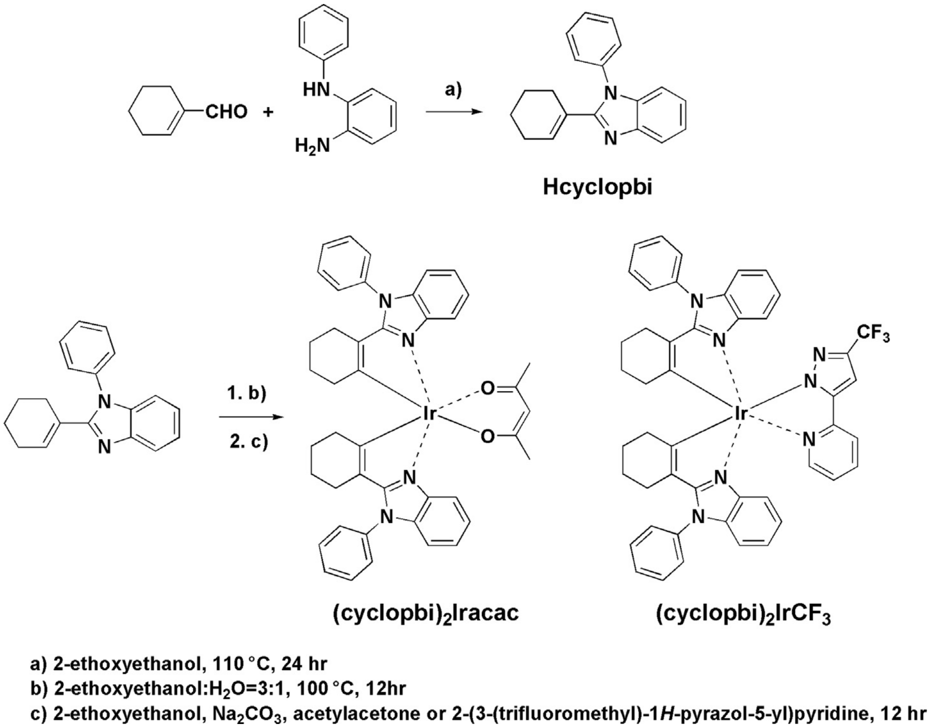

a) 2-ethoxyethanol, 110 °C, 24 hr
b) 2-ethoxyethanol:H_2O=3:1, 100 °C, 12hr
c) 2-ethoxyethanol, Na_2CO_3, acetylacetone or 2-(3-(trifluoromethyl)-1*H*-pyrazol-5-yl)pyridine, 12 hr

Scheme 1. Synthetic routes of cyclometalated ligand Hcyclopbi and bis-cyclometalated iridium complexes (cyclopbi)$_2$Iracac and (cyclopbi)$_2$IrCF$_3$.

The dimer complex, 2.0 mmol acetylacetone, 4.0 mmol Na_2CO_3 and 15 ml 2-ethoxyethanol were charged into a round bottomed flask, the mixture was then refluxed under an argon atmosphere for another 12 h. After cooling to room temperature, the precipitate was filtered off and washed with water, ethanol and ether, respectively. The crude product was purified by silica column chromatography with dichloromethane/petroleum ether (1:10, v/v) as eluent to give 0.55 g **(cyclopbi)$_2$Iracac** as an orange powder. Yield: 65.6%. ^{1}H NMR ($CDCl_3$, 600 MHz): δ = 7.5581–7.4978 (m, 10 H), 7.4395 (d, J = 8.04 Hz, 2 H), 7.1961 (t, J = 7.98 Hz, 2 H), 7.0955 (t, J = 7.98 Hz, 2 H), 6.9799 (d, J = 8.04 Hz, 2 H), 5.1585 (s, 1 H), 1.8574 (s, 6 H), 1.9098–1.7802 (m, 4 H), 1.6122–1.5701 (m, 4 H), 1.4554–1.4328 (m, 4 H), 1.2735–1.2556 (m, 4 H); ^{13}C NMR ($CDCl_3$, 150 MHz): δ = 184.39, 178.14, 167.91, 141.15, 136.37, 135.80, 129.27, 129.08, 128.86, 128.73, 128.21, 122.93, 120.45, 120.19, 114.33, 109.34, 101.10, 36.45, 28.56, 26.39, 23.58, 23.07; HRMS (APCI): m/z calcd for $C_{43}H_{41}IrN_4O_2$: 838.2859; found: 838.2871.

2.3.3. Bis[2-cyclohexenyl-1-phenyl-1H-benzo[d]imidazole][2-(3-(trifluoromethyl)-1H-pyrazol-5-yl)pyridinate]iridium(III) [(cyclopbi)$_2$IrCF$_3$]

The synthetic procedure for **(cyclopbi)$_2$IrCF$_3$** was similar to that of **(cyclopbi)$_2$Iracac**, except that 2.0 mmol 2-(3-(trifluoromethyl)-1*H*-pyrazol-5-yl)pyridine was used instead of acetylacetone. The crude product was purified by silica column chromatography with dichloromethane/petroleum ether (1:10, v/v) as eluent to give 0.52 g **(cyclopbi)$_2$IrCF$_3$** as a yellow powder. Yield: 55%. ^{1}H NMR ($CDCl_3$, 600 MHz): δ = 8.3850 (d, J = 5.22 Hz, 1 H), 7.7336–7.4262 (m, 11 H), 7.3395 (m, 1 H), 7.1294 (t, J = 6.06 Hz, 1 H), 6.9674–6.8943 (m, 4 H), 6.8601 (d, J = 7.86 Hz, 1 H), 6.8005–6.7478 (m, 2 H), 5.8529 (d, J = 7.92 Hz, 1 H), 5.6751 (d, J = 8.1 Hz, 1 H), 1.9276–1.2584 (m, 16 H); ^{13}C NMR ($CDCl_3$, 150 MHz): δ = 183.58, 181.12, 167.99, 167.33, 156.75, 150.99, 150.27, 140.59, 139.74, 137.04, 136.12, 136.08, 135.94, 135.55, 129.46, 129.34, 129.21, 129.00, 128.96, 128.92, 128.68, 128.30, 128.06, 123.50, 122.53, 121.93, 121.75, 121.00, 120.40, 119.65, 119.19, 114.81, 112.27, 109.89, 109.27, 102.29, 35.88, 34.95, 26.82, 26.57, 23.82, 23.57, 23.47, 23.36; HRMS (APCI): m/z calcd for $C_{47}H_{39}F_3IrN_7$: 951.2848; found: 951.2901.

3. Results and discussion

3.1. Photophysics characteristics

The UV–Vis and photoluminescence (PL) spectra of complexes (cyclopbi)$_2$Iracac and (cyclopbi)$_2$IrCF$_3$ in dichloromethane were shown in Fig. 1. For complex (cyclopbi)$_2$Iracac, the absorption before 352 nm was attributed to the π–π* transition of ligand Hcyclopbi, while from 352 to 524 nm was the characteristic of metal to ligand charge transfer (MLCT) absorption of iridium complexes similar to those reported previously [22,23]. For complex (cyclopbi)$_2$IrCF$_3$, the π–π* transition absorption was much stronger than that of (cyclopbi)$_2$Iracac because of the blend π–π*

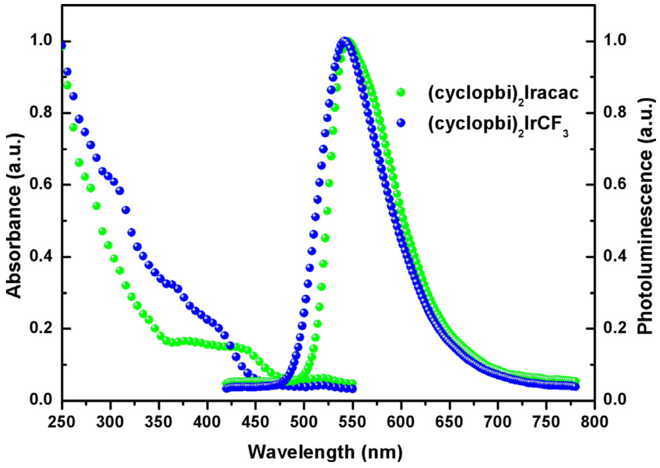

Fig. 1. UV–Vis and PL spectra of complexes (cyclopbi)$_2$Iracac and (cyclopbi)$_2$IrCF$_3$ in dichloromethane solution.

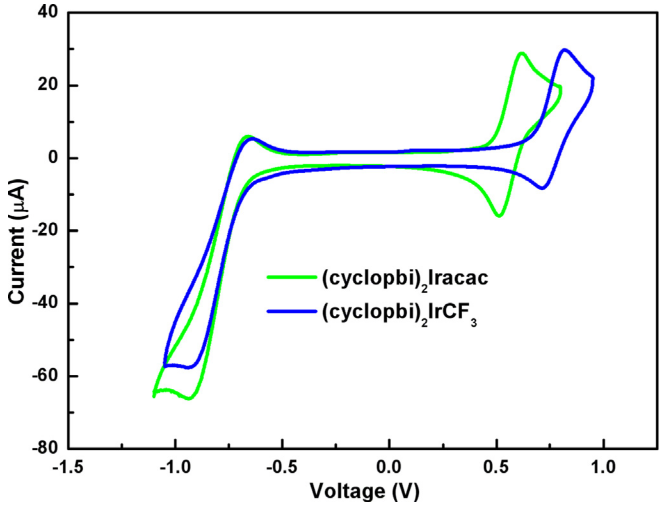

Fig. 2. Cyclic voltammetry curves of (cyclopbi)$_2$Iracac and (cyclopbi)$_2$IrCF$_3$ in dichloromethane solution.

transition of Hcyclopbi and 2-(3-(trifluoromethyl)-1*H*-pyrazol-5-yl)pyridine ligand. The blue shifted singlet MLCT (^{1}MLCT) absorption band of complex (cyclopbi)$_2$IrCF$_3$ compared to (cyclopbi)$_2$Iracac was mainly because of the stronger electron withdrawing property of 2-(3-(trifluoromethyl)-1*H*-pyrazol-5-yl) pyridine than acetylacetone, which led to higher energy MLCT state and blue-shifted photoluminescence [23–26]. However, the triplet MLCT (^{3}MLCT) absorption of the two complexes was same at 518.2 nm. Both the complexes show strong greenish yellow phosphorescence at room temperature in dichloromethane solution with peak wavelength 545 and 542 nm, respectively. The PL quantum yields (φ) of (cyclopbi)$_2$Iracac and (cyclopbi)$_2$IrCF$_3$ were calculated to be 0.22 and 0.25, respectively, with *fac*-Ir(ppy)$_3$ as the standard.

3.2. Electrochemistry characteristics

Fig. 2 depicts the cyclic voltammograms of the two complexes. The onset oxidation (E_{ox}) of (cyclopbi)$_2$Iracac and (cyclopbi)$_2$IrCF$_3$ were 0.49 and 0.68 V, respectively, which were usually considered as the metal-centered couple i.e. IrIII/IrIV of the complexes [27,28]. The oxidation and reduction onset of ferrocene were 0.47 and 0.29 V, respectively, then the HOMO of (cyclopbi)$_2$Iracac and (cyclopbi)$_2$IrCF$_3$ were estimated to be −4.91 and −5.10 eV, respectively, according to the previously reported method [29]. In cyclometalated iridium complexes, the HOMO energy level normally localized on the metal and cyclometalated ligand, and because of the stronger electron donating ability of cyclohexenyl than styryl, the HOMO of (cyclopbi)$_2$Iracac was higher than −5.11 eV of reported (psbi)$_2$Iracac [18]. (cyclopbi)$_2$IrCF$_3$ exhibit low HOMO compared to (cyclopbi)$_2$Iracac was the result of strong electron withdrawing ability of 2-(3-(trifluoromethyl)-1*H*-pyrazol-5-yl) pyridine compared to acetylacetone. The optical band gaps (E_g) of (cyclopbi)$_2$Iracac and (cyclopbi)$_2$IrCF$_3$ were calculated about 2.28 and 2.20 eV, as a result the LUMO were calculated from HOMO and E_g, estimated to be −2.63 and −2.90 eV, respectively. For (cyclopbi)$_2$Iracac, the LUMO was only contributed by the π orbital of the cyclometalated ligand cyclopbi and independent of the ancillary ligand, however, the 2-(3-(trifluoromethyl)-1*H*-pyrazol-5-

Table 1
Photophysics and electrochemistry characteristics of complexes (cyclopbi)$_2$Iracac and (cyclopbi)$_2$IrCF$_3$ in dichloromethane solution.

Complex	Absorption (nm)	PL (nm)	φ	E_{ox} (V)	E_g (eV)	HOMO (eV)	LUMO (eV)
(cyclopbi)$_2$Iracac	279.7, 378.3, 437.9, 518.2	545	0.22	0.49	2.28	−4.91	−2.63
(cyclopbi)$_2$IrCF$_3$	306.1, 364.1, 411.6, 518.2	542	0.25	0.68	2.20	−5.10	−2.90

Table 2
Electroluminescence characteristics of complexes (cyclopbi)$_2$Iracac and (cyclopbi)$_2$IrCF$_3$ with different doping concentration, (ppy)$_2$Iracac was used as reference.

Complex	Doping concentration (wt%)	EL (nm)	U_{on}[a] (V)	η_c[b] (cd/A)	Brightness[c] (cd/m^2)	CIE (*x*, *y*)[d]
(cyclopbi)$_2$Iracac	8	537, 561	5.4	22.3	16,300	0.42, 0.56
	12	540, 565	5.3	22.1	14,100	0.42, 0.55
(cyclopbi)$_2$IrCF$_3$	8	550	6.5	12.9	4200	0.40, 0.56
	12	552	6.6	9.2	4400	0.41, 0.56
(ppy)$_2$Iracac	8	520	5.3	16.9	29,000	0.31, 0.63
	12	520	5.8	26.4	20,700	0.31, 0.63

[a] Turn on voltage.
[b] Maximum current efficiency.
[c] Maximum brightness.
[d] CIE at 8 V.

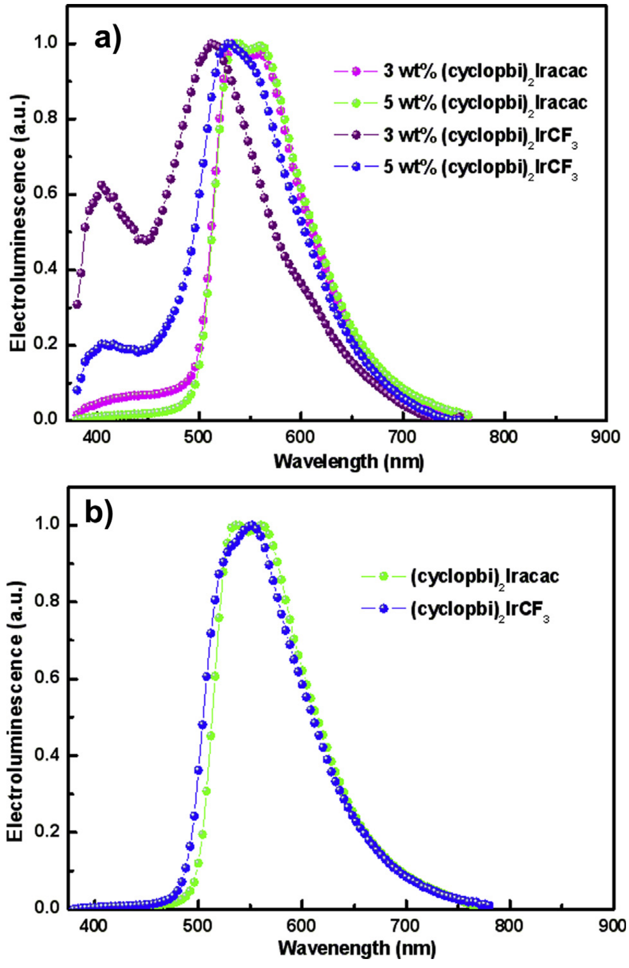

Fig. 3. EL spectra of devices based on (cyclopbi)$_2$Iracac and (cyclopbi)$_2$IrCF$_3$. a) With doping concentration 3 wt% and 5 wt% at 8 V; b) With doping concentration 8 wt% at 8 V.

yl) pyridine ligand decreased the HOMO and LUMO of (cyclopbi)$_2$IrCF$_3$ significantly. The photophysics and electrochemistry characteristics of complexes (cyclopbi)$_2$Iracac and (cyclopbi)$_2$IrCF$_3$ were summarized in Table 1.

3.3. Electroluminescence characteristics

In order to explore the EL characteristics of (cyclopbi)$_2$Iracac and (cyclopbi)$_2$IrCF$_3$, multi-layer devices were fabricated as ITO/m-MTDATA (10 nm)/NPB (20 nm)/CBP:iridium complexes (30 nm)/TPBi (30 nm)/LiF/Al. NPB was used as HTL, CBP was selected as host because of the good overlap of the absorption of iridium complexes and the PL of CBP (380 nm) [30], TPBi was used as electron transporting and exciton blocking layer followed by LiF and Al as cathode. As a comparison, (ppy)$_2$Iracac was employed with doping concentration 8 and 12 wt%.

The doping concentration was optimized from 3 wt%, 5 wt% to 8 wt% and 12 wt%, among which the device characteristics containing 8 and 12 wt% emitters in the EML were summarized in Table 2. Fig. 3a shows the EL spectra of (cyclopbi)$_2$Iracac and (cyclopbi)$_2$IrCF$_3$ at doping concentration 3 wt% and 5 wt%, respectively. Being as expected CBP emission was obtained for 3 wt % doped (cyclopbi)$_2$Iracac and 3 wt%, 5 wt% doped (cyclopbi)$_2$IrCF$_3$ because of the incompletely Dexter energy transfer from host to dyes caused by the low doping concentration. The EL spectra around 410 nm were stronger for (cyclopbi)$_2$IrCF$_3$ compared to (cyclopbi)$_2$Iracac at corresponding doping concentration was due to the delocalized HOMO of (cyclopbi)$_2$IrCF$_3$ which make a large barrier for hole injection from NPB to the emitter. When the doping concentration increased to 8 and 12 wt%, pure greenish yellow phosphorescence was obtained for both the devices (Fig. 3b). For (cyclopbi)$_2$Iracac, the EL spectra show vibration structure with two peak wavelength 537 and 561 nm at 8 wt% doping concentration, slightly red shift was obtained when the doping concentration improved to 12 wt%, the CIE changed from (0.42, 0.56) to (0.42, 0.55) which was measured at 8 V respectively as summarized in Table 2. For (cyclopbi)$_2$IrCF$_3$, the peak wavelength was 550 nm with CIE (0.40, 0.56) at doping concentration 8 wt% under applied voltage 8 V.

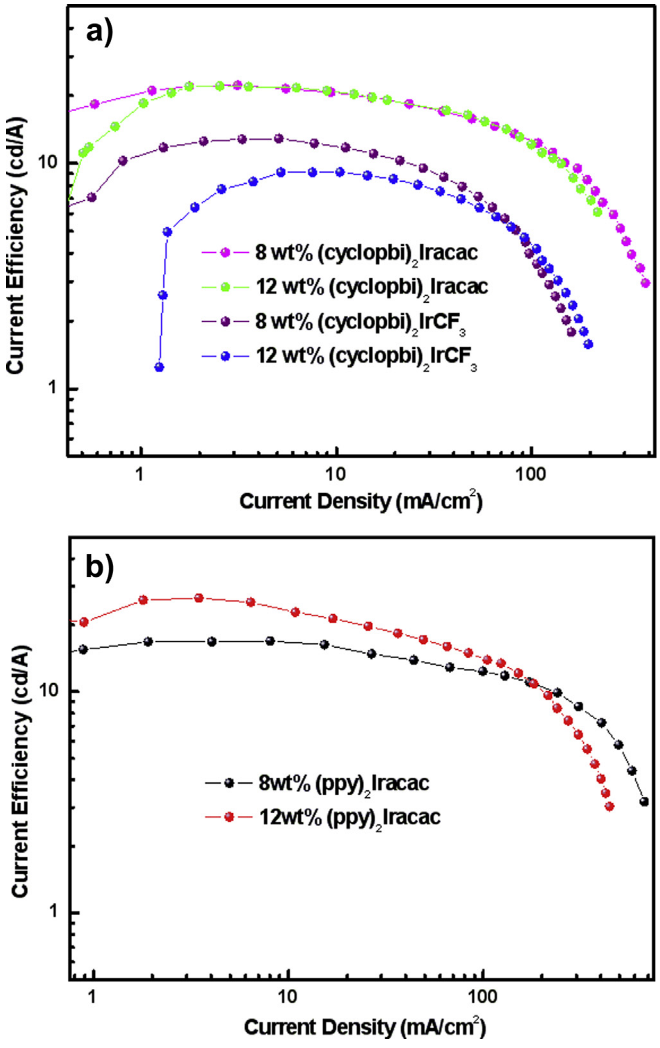

Fig. 4. Current efficiency versus current density of devices based on (cyclopbi)$_2$Iracac, (cyclopbi)$_2$IrCF$_3$ and (ppy)$_2$Iracac with doping concentration 8 wt% and 12 wt%, respectively. a) (cyclopbi)$_2$Iracac and (cyclopbi)$_2$IrCF$_3$; b) (ppy)$_2$Iracac.

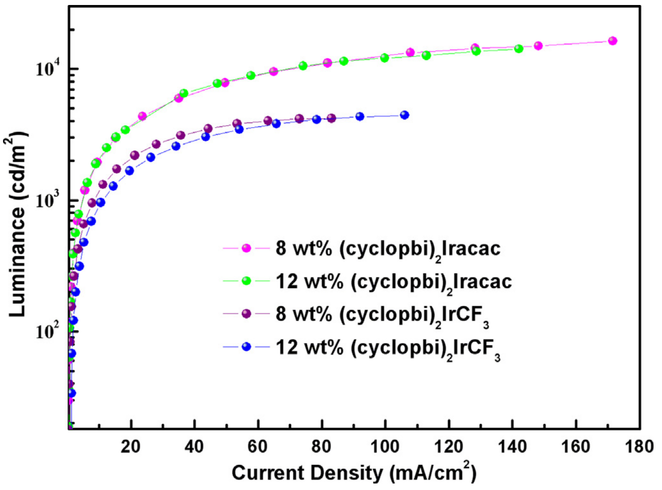

Fig. 5. Luminance versus current density relationship of (cyclopbi)$_2$Iracac and (cyclopbi)$_2$IrCF$_3$ with doping concentration 8 wt% and 12 wt%, respectively.

Fig. 4a shows the η_c and current density relationship of (cyclopbi)$_2$Iracac and (cyclopbi)$_2$IrCF$_3$ with doping concentration 8 and 12 wt% respectively, the maximum η_c of 8 wt% doped (cyclopbi)$_2$Iracac device was 22.3 cd/A at current density 3.1 mA/cm^2, which was comparable to that of (ppy)$_2$Iracac (Fig. 4b). When the doping concentration increased to 12 wt%, maximum η_c 22.1 cd/A was still maintained indicating nearly no concentration quenching. However, efficiency dropped significantly because of the strong concentration quenching [31–33]. As described in Table 2, the turn on voltage of device employed 8 wt% (cyclopbi)$_2$Iracac was much lower than that of (cyclopbi)$_2$IrCF$_3$ as the result of the high HOMO energy of (cyclopbi)$_2$Iracac which can balance the hole and electron in the EML. The maximum brightness of 8 wt% (cyclopbi)$_2$Iracac doped device was 16,300 cd/m^2, 14,100 cd/m^2 was obtained when the doping concentration increased to 12 wt% as described in Fig. 5. The brightness of (cyclopbi)$_2$IrCF$_3$ based devices was relatively lower than that of (cyclopbi)$_2$Iracac may be resulted from the high drive voltage caused by the unbalanced hole and electron mobility in the EML.

4. Conclusions

In conclusion, 2-cyclohexenyl-1-phenyl-1*H*-benzo[*d*]imidazole and its iridium complexes (cyclopbi)$_2$Iracac and (cyclopbi)$_2$IrCF$_3$ were designed and synthesized for the first time. Photophysics, electrochemistry and electroluminescence characteristics were investigated and high efficiency greenish yellow OLEDs with maximum η_c 22.3 cd/A and maximum brightness 16,300 cd/m^2 was obtained employing (cyclopbi)$_2$Iracac as the emitter, which was comparable to that of traditional phosphorescent dye (ppy)$_2$Iracac. We thought the higher energy level of cyclohexenyl compared to that of phenyl and the excellent electron transporting ability of benzoimidazole lead to easily hole injecting and balanced electron and hole mobility in the emitting layer, which may helpful for designing efficiency phosphores. On the other hand, it's important to develop greenish yellow phosphorescence dyes for white OLEDs designing and explore their potential application in solid-state lighting and display.

Acknowledgment

This work was supported by Outstanding Young Scientists Research Award Fund of Shandong Province (BS2010NJ021), Shandong Provincial Natural Science Foundation (ZR2011BZ007), Qingdao Municipal Science and Technology Program (11-2-4-22-hz), and State Key Laboratory of Luminescent Materials and Devices (South China University of Technology). We thank Dr. Xiao Li and Haijun Chi for the NMR analysis in University of Science and Technology Liaoning.

References

[1] Ho PKH, Kim JS, Burroughes JH, Becker H, Li SFY, Brown TM, et al. Nature 2000;404:481.
[2] Gu G, Parthasarathy G, Forrest SR. Appl Phys Lett 1999;74:305.
[3] Wu CC, Chen CW, Cho TY. Appl Phys Lett 2003;83:611.
[4] Baldo MA, O'Brien DF, You Y, Shoustikov A, Sibley S, Thompson ME, et al. Nature 1998;395:151.
[5] Adachi C, Baldo MA, Thompson ME, Forrest SR. J Appl Phys 2001;90:5084.
[6] Ikai M, Tokito S, Sakamoto Y, Suzuki T, Taga Y. Appl Phys Lett 2001;9:156.
[7] Lamansky S, Djurovich P, Murphy D, Razzaq FA, Lee HE, Adachi C, et al. J Am Chem Soc 2001;123:4304.
[8] Wang Q, Chen YH, Chen JS, Ma DG. Appl Phys Lett 2012;101:133302.
[9] Baldo MA, Lamansky S, Burrows PE, Thompson ME, Forrest SR. Appl Phys Lett 1999;75:4.
[10] Paulose BMJS, Rayabarapu DK, Duan JP, Cheng CH. Adv Mater 2004;16:2003.
[11] Rayabarapu DK, Paulose BMJS, Duan JP, Cheng CH. Adv Mater 2005;17:349.
[12] Liu T, Zhou X, Pan QJ, Xia BH, Zhang HX. J Organomet Chem 2009;694:150.
[13] Han LL, Yang DF, Li WL, Chu B, Chen YR, Su ZS, et al. Appl Phys Lett 2006;94:163303.
[14] Xiao GY, Lei P, Chi HJ, Lu YH, Dong Y, Hu ZZ, et al. Synth Met 2009;159:705.
[15] Huang WS, Lin JT, Chien CH, Tao YT, Sun SS, Wen YS. Chem Mater 2004;16:2480.
[16] Wang Q, Tao YT, Qiao XF, Chen JS, Ma DG, Yang CL, et al. Adv Funct Mater 2011;21:1681.
[17] Ding JQ, Gao J, Cheng YX, Xie ZY, Wang LX, Ma DG, et al. Adv Funct Mater 2006;16:575.
[18] Zhang GH, Wu FI, Jiang XQ, Sun PP, Cheng CH. Synth Met 2010;160:1906.
[19] Kang DM, Kang JW, Park JW, Jung SO, Lee SH, Park HD, et al. Adv Mater 2008;20:2003.
[20] Park YS, Kang JW, Kang DM, Park JW, Kim YH, Kwon SK, et al. Adv Mater 2008;20:1957.
[21] Takiguchi T, Okada S, Tsuboyama A, Noguchi K, Moriyama T, Kamatani J, et al. US Patent 20020094453A1, 2002.
[22] Ho CL, Wang Q, Lam CS, Wong WY, Ma DG, Wang LX, et al. Chem Asian J 2009;4:89.
[23] Chou PT, Chi Y. Chem Eur J 2007;13:380.
[24] Yang CH, Li SW, Chi Y, Cheng YM, Yeh YS, Chou PT, et al. Inorg Chem 2005;44:7770.
[25] Yeh YS, Cheng YM, Chou PT, Lee GH, Yang CH, Chi Y, et al. ChemPhysChem 2006;7:2294.
[26] Chang CF, Cheng YM, Chi Y, Chiu YC, Lin CC, Lee GH, et al. Angew Chem Int Ed Engl 2008;47:4542.
[27] Deng LJ, Zhang T, Wang RJ, Li JY. J Mater Chem 2012;22:15910.
[28] Su HC, Fang FC, Hwu TY, Hsieh HH, Chen HF, Lee GH, et al. Adv Funct Mater 2007;17:1019.
[29] Li YF, Cao Y, Gao J, Wang DL, Yu G, Heeger AJ. Synth Met 1999;99:243.
[30] Adamovich V, Brooks J, Tamayo A, Alexander AM, Djurovich PI, D'Andrade BW, et al. New J Chem 2002;26:1171.
[31] Zhang YQ, Zhong GY, Cao XA. J Appl Phys 2010;108:083107.
[32] Kawamura Y, Brooks J, Brown JJ, Sasabe H, Adachi C. Phys Rev Lett 2006;96:017404.
[33] Divayana Y, Sun XW. Phys Rev Lett 2007;99:143003.